Printed Packaging Authentication: Similarity Metric Learning for Rotogravure Manufacture Process Identification

Tetiana Yemelianenko, Alain Trémeau, Iuliia Tkachenko

Printed packaging authentication: similarity metric learning for rotogravure manufacture process identification

Tetiana Yemelianenko[1], Alain Trémeau[2] and Iuliia Tkachenko[1]
[1]*Univ Lyon, Univ Lyon 2, CNRS, INSA Lyon, UCBL, LIRIS, UMR 5205, F-69676 Bron, France*
[2]*Univ. Lyon, UJM-Saint-Etienne, Laboratoire Hubert Curien UMR CNRS 5516, F-42023 St-Etienne, France*
iuliia.tkachenko@liris.cnrs.fr

Keywords: Rotogravure Press Identification, Press Forensics, Printed support forensics, Medicine Blister Authentication

Abstract: The number of medicine counterfeits increases each year due to the accessibility of printing devices and the weak protection of medicine blister foils. The medicine blisters are often produced using the rotogravure printing process. In this paper, we address the problem of rotogravure press identification and printed support identification using similarity metric learning. Both identification problems are difficult as the impact of printing press or of printing support are minimal, moreover the classical techniques (for example, the use of Pearson correlation) cannot identify the rotogravure press or the printing support used for the packaging production. We show that the similarity metric learning can easily identify the press used and the printing support used. Additionally, we explore the possibility to use the proposed approach for packaging authentication.

1 INTRODUCTION

The World Health Organization argues that 1-in-10 medicines in lower-and middle-income countries are falsified or substandard[1]. This fact is worrying as the medicine counterfeits may have a significant impact on human health and life.

Unfortunately the existing anti-counterfeiting techniques are either too expensive to be inserted in the medicine packaging or too complicated to be verified by non-professionals. Additionally, due to international regulations and costs, the pharmaceutical companies prefer to use a minimal graphical design (Davison, 2011). Finally, due to big printing amounts, the majority of medicine packaging is printed using the rotogravure printing process, that is one of the cheapest and fasten processes.

The rotogravure printing process has some specific characteristics that can be used in forensics (Tkachenko et al., 2019; Tkachenko et al., 2020). Therefore, the forensics based solutions are very promising and can easily be used to protect and to authenticate pharmaceutical printed packaging.

One of such solutions, developed for authentication of medicine blister foils printed using rotogravure process, is based on the use of a regular test pattern (Tkachenko et al., 2022). Thanks to this regular test pattern, the authors showed that it is possible to identify medicine packaging printed using a specific cylinder engraving process (engraved using chemical etching, see Section 2 for more details). The authors used two approaches based on Pearson correlation and Non-Negative Least Squares (NNLS) classifier to identify a set of samples printed using two chemically engraved cylinders. Nevertheless, it was shown that these approaches cannot differentiate samples printed using a same engraved cylinder but with different presses.

In this paper, we want to explore this problem, i.e. the identification of rotogravure press used. We propose to use the similarity metric learning (Duffner et al., 2021), which has shown its efficiency in biometric applications (as face and signature identification) for rotogravure press identification. The contributions of this paper are the following:

1. We explored the efficiency of similarity metric learning for the rotogravure printing process forensics.
2. We enlarged the database introduced in (Tkachenko et al., 2022) by adding samples printed on strips using electro-mechanically engraved cylinder[2]. To the best of our knowledge,

[1]https://apps.who.int/iris/bitstream/handle/10665/270662/PMC2855605.pdf?sequence=1&isAllowed=y

[2]The data set is publicly available at https://gitlab.liris.cnrs.fr/rotogravure-printing/regular-pattern-dataset.

electro-mechanical samples have never be considered in other studies in the field of medicine blister authentication.

3. We studied the impact of electro-mechanical engraving process, and the possibility to identify the press used, from a set of samples printed using electro-mechanically engraved cylinders. It is a quite challenging case, as the electro-mechanical engraving process is well controlled and, thus, printed samples have less individual imperfections.
4. We studied the impact of the printing support used (strip - thicker aluminium foil and blister - thinner aluminium foil). We explored the possibility to identify the printing support while the engraved cylinder and the rotogravure press are identical.

The rest of this paper is organized as follows. The description of the rotogravure printing process and its characterization are discussed in Section 2. The proposed identification system is presented in Section 3. The experimental results are shown in Section 4. We discuss the possibility to use the proposed identification approach for packaging authentication in Section 5. Finally, we conclude this work in Section 6.

2 ROTOGRAVURE PRINTING PROCESS

Rotogravure printing is currently used for packaging manufacturing thanks to its fast and relatively cheap printing process. The rotogravure printing process differs a lot from other printing processes commonly used (using for example laser or inkjet printers).

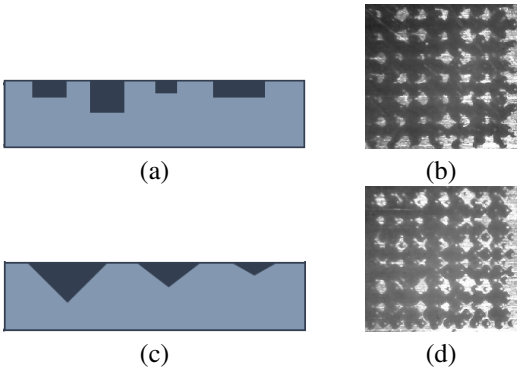

Figure 1: An illustration of: a) a cylinder engraved by chemical etching; b) a regular test pattern (P_1C_1s) printed using a chemically engraved cylinder; c) a cylinder engraved by electro-mechanical etching; d) a regular test pattern (P_1M_1s) printed using a cylinder engraved by electro-mechanical etching.

To print a packaging using the rotogravure printing process, we need to follow the following steps:

1. Design an artwork considering specific engraving parameters (as width of lines, dot shapes, color orders, etc.) and using a specific graphic editor software.
2. Engrave a cylinder using the designed artwork. Depending of the type of engraving process (chemical etching, electro-mechanical or laser engraving), the shape of printed dots and the quality of images will differ. For example, the sharpness of edges in electro-mechanical engraving is ensured by the cells with different depths and areas, meanwhile all cells have the same pyramid shape (see Fig. 1.c). In the case of chemical etching, sharper edges are obtained thanks to engraved half-dots (see Fig. 1.a).
3. Print the artwork on a chosen support using the engraved cylinder. The rotogravure printing process is split on color units. One color unit, illustrated in Fig 2, consists of an engraved cylinder, a press and a pan of ink. After the ink transfer from cylinder cells to the printing support, the ink is dried using high velocity air nozzle dryer.

More details about the rotogravure printing process can be found in (Kipphan, 2001). Rotogravure printing has some particular characteristics and imperfections (Tkachenko et al., 2019) that can be used in manufacturing process identification (Tsai et al., 2019; Joshi et al., 2020) and packaging authentication (Nguyen et al., 2021). In this paper, we propose to use the regular test pattern introduced in (Tkachenko et al., 2022) printed using cylinders engraved by chemical etching (Fig. 1.b) and using electro-mechanically engraved cylinders (Fig. 1.d).

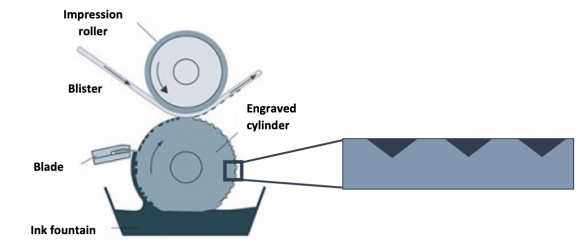

Figure 2: The printing process using rotogravure. Cylinder cells illustrated correspond to a electro-mechanical engraving.

3 PROPOSED IDENTIFICATION SYSTEM

Previously, it was shown that the cylinder signature is the parameter which most impacts the artworks printed by a rotogravure process (Tkachenko et al., 2020). It was also demonstrated that the identification of the cylinder(s) used can be done using the Pearson correlation or the NNLS classification. Nevertheless, according to (Tkachenko et al., 2022), it is not possible to identify the press used to print an artwork on a packaging, as well as to identify the support used for the printing, using these metrics.

The current advances in deep learning techniques make possible a quick identification of people (using facial biometrics or handwritten signatures). (Tsai et al., 2019) showed that printer identification can be also efficiently performed using deep learning techniques. In this context, we propose to use the similarity metric learning for rotogravure press identification.

In the following sections, we introduce first the two identification scenarios studied, next the Siamese Neural Network used, and lastly the training setup used for rotogravure press and support identification.

3.1 Identification scenarios studied

To authenticate a medicine packaging, we need to verify the authenticity of the manufacturing process used to print it (Schraml et al., 2017; Schraml et al., 2018). The objective is to check that the cylinder, the press and the support used to print this packaging come from an authorized manufacture. The identification of rotogravure cylinders used to print pharmaceutical packaging was solved in (Tkachenko et al., 2022). The next step now is to study the two following identification problems:

- The identification of the press used: This scenario happens when we need to identify a rotogravure press to ensure that some samples were printed by an authentic printing company.
- The identification of the printing support used: This scenario allows us to verify the authenticity of the printing support used for packaging.

In this paper, we want to solve these two identification problems using a Siamese Neural Network with triplet loss.

3.2 Siamese Neural Network used

Deep learning networks are very powerful for supervised learning when a large amount of data is available. However, in the majority of real-world applications, it is very difficult and expensive to collect big data sets. Therefore, weakly-supervised or semi-supervised learning approaches are very popular today. One of such approaches is the similarity metric learning that learns to differentiate the inputs of the model instead of classifying them (Duffner et al., 2021).

When we talk about similarity metric learning, the commonly used models are based on Siamese Neural Networks (SNN). SNN were proposed in (Bromley et al., 1993) for solving the task of signature verification. The SNN consists of twin neural networks which receive two different inputs, meanwhile these parallel neural networks share the same parameters. Each neural network produces embeddings which are united with the top conjoining distance layer, based on the distance loss function which represents the similarity between inputs.

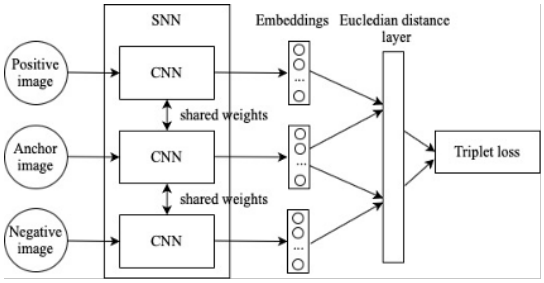

Figure 3: The SNN architecture used.

In this paper, we use the triplet SNN which is composed of three identical sub-networks (see Fig. 3), to solve the task of press identification. This model uses three images for the input (A,P,N): an anchor A (template image), a positive sample P (image printed with the same conditions as the template) and a negative sample N (image printed with different manufacturing conditions - another press, cylinder or support used). The model was trained to minimize the distance between similar images and to maximize the distance between dissimilar images. For this purpose, we used a triplet loss function (Weinberger et al., 2005) defined by the following Euclidean distance function :

$$L(A,P,N) = \max(||e(A)-e(P)||^2 - ||e(A)-e(N)||^2 + \alpha), \quad (1)$$

where α is the margin between positive and negative pairs, and $e(x)$ is the embedding.

For the training the standard stochastic gradient descent was used. The accuracy of the model was calculated as a binary accuracy, based on the similarity between the anchor and the positive images, in comparison with the similarity between the anchor and the negative images.

3.3 Training setup used

Due to the relatively small size of the training data set, we decided to use a transfer learning approach. This approach is based on the use of a pre-trained model. The main objective was to use the trained layers of a pre-trained model, freezing the weights of this model, then adding several trainable layers on the top of frozen layers, and lastly training them. The new train model can be used for feature extraction. Fine-tuning was used to improve the efficiency of the model, it consists in: unfreezing several top layers of the model, and re-training them with a small learning rate. For the feature extraction, we used two deep convolutional networks: VGG16 (Simonyan and Zisserman, 2015) and ResNet50 (He et al., 2016), pre-trained on Imagenet data set (consisting of 1.4M images and 1000 classes):

- VGG16 model has 13 convolutional layers, five max pooling layers, and three dense layers. The specificity of this architecture comes from the use of very small 3×3 convolution filters.
- ResNet50 is a very deep CNN architecture with 50 layers. The specificity of this architecture comes from the bottleneck design of the building blocks, which reduces the number of parameters and matrix multiplications, this enables to speed the training of each layer.

In our identification process, both models (VGG16 and ResNet50) were only used for feature extraction, and the last classification layers were removed from these models.
We added to each pre-trained model: 1) three dense layers (the first dense layer with 1024 neurons, the two following layers with 512 neurons); 2) one dropout layer with a learning rate equals to 0.2; and 3) one batch normalization layer. The output layer for both models consists of 512 neurons, which represents the extracted features. These outputs were used for calculating the distances between the anchor and positive images, and also between the anchor and negative images. Then, the model was trained to minimize the triplet loss function (1). After a series of experiments, the value of the margin parameter α was set to 0.2, meanwhile the learning rate was set to 0.0001. For fine-tuning, the fifth block was unfreezed in both models.

4 EXPERIMENTAL RESULTS

In this section, we will present the experimental results. First, we present the augmented data set used in our experiments, next we discuss the results obtained for rotogravure and printing support identification.

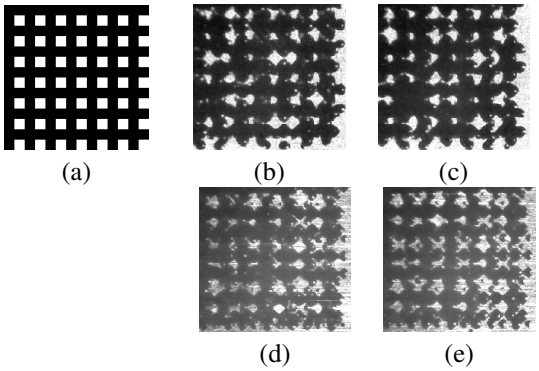

Figure 4: An illustration of: a) the regular test pattern E used; b-c) two regular test patterns printed on blister, using a chemical etching engraved cylinder; d-e) two regular test patterns printed on strip, using an electro-mechanically engraved cylinder.

4.1 Database description

In this paper, we worked with a regular test pattern E (see Fig. 4.a) printed using two presses (P_1 and P_2) and two types of engraving cylinders: 1) two cylinders engraved using chemical etching (C_1 and C_2); and 2) a cylinder engraved using electro-mechanical process (M_1). The samples printed using the cylinders engraved using chemical etching (Fig. 4.b-c) differ a lot from the samples printed using the electro-mechanically engraved cylinder (Fig. 4.d-e).
Additionally, we studied the impact of the printing support used, using the regular test patterns printed on: 1) thin aluminium foils - called blisters (letter 'b' in the tables and figures); and 2) thick aluminium foils - called strips (letter 's' in the tables and figures). The details about the data set used are given in Table 1.

	E_1	E_2	E_3	E_4	E_5	E_6
Chemical etching						
P_1C_2s	50	50	50	50	50	50
P_2C_2s	50	50	50	50	50	50
P_1C_1b	50	50	50	50	50	50
P_2C_1b	50	50	50	50	50	50
Electro-mechanical engraving						
P_1M_1s	50	50	50	50	50	50
P_2M_1s	49	48	49	48	49	48

Table 1: Description of the database used (specifically designed for this study) with a regular pattern printed in different positions ($E_i, i = 1,\ldots,6$) on the cylinder, printed with different types of engraving processes on different printing supports.

The subsets P_1C_2s, P_2C_2s, P_1C_1b, P_2C_1b were already introduced in (Tkachenko et al., 2022). In this new study, we enlarged this database by adding the subsets P_1M_1s and P_2M_1s for the purpose of the evaluation of identification scenarios discussed in Section 3.1. All images of the regular test pattern were captured using an USB-microscope[3] with $\times 5$ magnification. The size of images is 432×452 pixels.
This database was divided in combinations of pairs: $P_1C_2s - P_2C_2s$, $P_1C_1b - P_2C_1b$ and $P_1M_1s - P_2M_1s$. Next, samples corresponding to each pair were split on training, validation, and test data set in the same way. We used 50% of images for the training set, 25% of images for the validation and test sets.
The triplets (anchor, positive, negative) were defined as follow: we created unique pairs (anchor, positive) from the first subset (for example, P_1M_1s), and we added a random image from the second subset (in our example, P_2M_1s) to each pair as a negative sample.
We used two approaches for making triplets. For the first strategy of splitting, we did not consider the regular test pattern position ($E_i, i = 1, \ldots, 6$) while preparing the triplets. For the second strategy, the regular test pattern position was taken into consideration.
All the involved networks were implemented using Python 3.6.2 with Keras 2.3.1 and TensorFlow 2.0.0.
The following sections report the results of experiments done for the validation of the proposed identification approach. We repeated each experiment 10 times with random splitting of the data set on train, test, and validation sets.

4.2 Identification of the press used

We evaluated the press identification task using three subsets of our database:

- Press identification while cylinders engraved using chemical etching and samples printed on strip (subsets P_1C_2s and P_2C_2s).
- Press identification while cylinders engraved using chemical etching and samples printed on blister (subsets P_1C_1b and P_2C_1b).
- Press identification while cylinders engraved using electro-mechanical engraving and samples printed on strip (subsets P_1M_1s and P_2M_1s).

The first series of experiments, illustrated by the results shown in Table 2 let us conclude that the use of ResNet50 network gives better results (in terms of accuracy) than VGG16 network. We can note that after fine-tuning, the ResNet50 model gives a little bit worse result in comparison with the model without fine-tuning, but if we consider the engraved position the results after fine-tuning are better.
Therefore, for all further experiments, we used only fine-tuned ResNet50 model trained with 20 epochs as the value of loss function in most cases did not change significantly after 15 epochs. To illustrate this, we plotted in Fig. 5 the training and validation accuracy curves for one of the experiments done.

	ResNet50		VGG16
	w/o pos.	w/pos.	
w/o fine-tuning	**0.9853**	0.9699	0.9398
w/ fine-tuning	0.9819	**0.9875**	0.9486

Table 2: Example of comparison of identification accuracy of images from subsets P_1M_1s and P_2M_1s, while using two training models, with and without fine tuning.

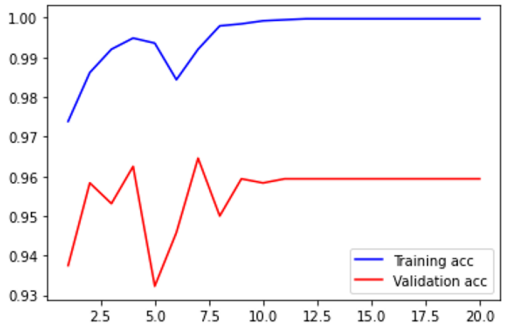

Figure 5: Training and validation accuracy curves for 20 training epochs.

Table 3 shows the obtained accuracy results of press identification. These results demonstrate that the similarity metric learning using ResNet50 for feature extraction based on the triplet loss can efficiently identify the rotogravure press used for packaging printing. It was shown that the printing position also impacts the printed image quality (Tkachenko et al., 2022). Therefore, we tested both strategies 1) without considering engraved position, and 2) considering engraved position. For the first strategy when we formed triplets for the "anchor-positive" pairs we did not consider engraved position, but for the second strategy we formed "anchor-positive" pairs only from the elements in one engraved position. Therefore, the training datasets are different in these two experiments.
The accuracy results in Table 3 prove that the consideration of engraved position can improve the identification accuracy (see Table 3 column 3). The worst results (identification accuracy equals to 0.88) are obtained for subsets P_1C_2s and P_2C_2s. One possible explanation is the big variability of training samples due to the complex standardization of chemical etching (Kipphan, 2001) and the higher complexity of print-

[3] Bodelin Proscope Microscope

ing support (strip aluminium foil has more surface imperfection than blister aluminium foil).

Subsets used	w/o position	w/ position
P_1C_2s vs P_2C_2s	0.8288	**0.8822**
P_1C_1b vs P_2C_1b	0.9576	**0.9610**
P_1M_1s vs P_2M_1s	0.9819	**0.9875**

Table 3: Press identification using ResNet50 with fine-tuning, while not considering or considering the position of regular test pattern on the cylinder.

4.3 Identification of the printing support used

In this experiment, we studied the impact of printing support for press identification. We used the subsets of images P_1C_1s and P_1C_1b, from (Tkachenko et al., 2022). While using the Pearson correlation, we cannot spot the differences between the images printed on blister and on strip. The results of this experiment are illustrated in Fig. 6.

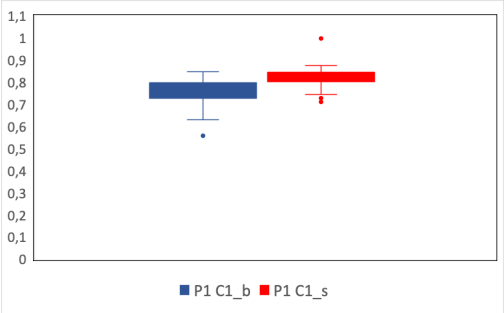

Figure 6: Press identification accuracy of samples printed on blister and on strip aluminum foils.

On the other hand, the proposed similarity metric learning model can successfully separate the samples that come from these subsets, as demonstrated in Fig. 7.

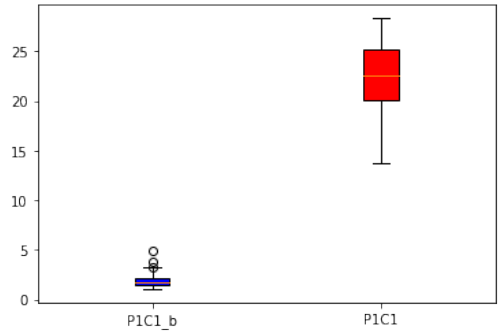

Figure 7: Press identification accuracy of samples printed on blister and on strip aluminum foils.

The results presented in previous sections illustrate the possibility to use SNN with triplet loss for the rotogravure manufacturing process identification.

5 Discussion about packaging authentication

Based on these results, we can conclude that it is possible to construct an authentication system using the proposed similarity metric learning approach. For this, we can empirically define a so called authentication threshold th (the maximal distance between the authentic templates used during training and validation samples). Then, we can use this threshold for authentication of test samples: if the minimal distance between a test sample and a template is smaller than th, then the test sample is considered as authentic.

	Actual	
Predicted	P_1C_1b	P_2C_1b
P_1C_1b	90.7%	9.3%
P_2C_1b	9.3%	90.7%

Table 4: Confusion matrix of samples authentication computed from data sets P_1C_1b and P_2C_1b.

We fixed experimentally the authentication threshold to th using the validation data set, and then classify the test images to authentic and fake classes. The confusion matrix, corresponding to some of the data sets studied, is presented in Tables 4- 6. From results shown in Tables 4- 5, we can conclude that it is possible to use the proposed similarity metric learning approach to efficiently authenticate the samples that were printed using the same engraved cylinder and two rotogravure presses.

	Actual	
Predicted	P_1M_1s	P_2M_1s
P_1M_1s	98.5%	3%
P_2M_1s	1.5%	97%

Table 5: Confusion matrix of samples authentication computed from data sets P_1M_1s and P_2M_1s.

The last experiment represents the situation, when falsified packaging follow the same manufacturing chain, but are printed on another printing support. Table 6 demonstrates that the proposed similarity metric learning approach can identify the printing support that was used for printing.
These results show the potential of the similarity metric learning for forensics and packaging authentication applications. Additionally, the use of relatively small data sets for training stage, motivates us to con-

	Actual	
Predicted	P_1C_1b	P_1C_1s
P_1C_1b	98.7%	2.7%
P_1C_1s	1.3%	97.3%

Table 6: Confusion matrix of sample authentication computed from data sets P_1C_1b and P_1C_1s.

tinue to study this approach for real-world authentication applications.

6 CONCLUSIONS

Medicine falsification is a big issue nowadays. We need to find simple and relatively cheap protection solutions. One of such solutions is the use of forensics approaches. To print pharmaceutical packaging printing manufactures use the rotogravure printing technique that has some specific characteristics. Previously, it was shown that the signature of the rotogravure cylinder can be easily identified using Pearson correlation. Nevertheless, the identification of the rotogravure press and of the printing support were shown to be a difficult problem. In this paper, we investigated the use of the similarity metric learning approach for these two identification scenarios.
Our experimental results prove the possibility to easily identify both the printing support used and the rotogravure press used for packaging pharmaceutical samples, using the similarity metric learning approach.
The next step will be to construct a full authentication system using the proposed similarity metric learning approach, and explore the possibility to use a smartphone camera for authentication.

ACKNOWLEDGEMENTS

We would like to thanks the PAUSE Program: Emergency Assistance to Ukrainian Researchers to support the scientific stay of T. Yemelianenko in LIRIS laboratory. This work was done in the context of the FakeNets project funded by Fédération Informatique de Lyon. All the printed samples were provided by Sergusa Solutions Pvt Ltd in the context of PackMark project (IFCPAR-7127) supported by the Indo-French Center for the Promotion of Advanced Research.

REFERENCES

Bromley, J., Guyon, I., LeCun, Y., Säckinger, E., and Shah, R. (1993). Signature verification using a" siamese" time delay neural network. *Advances in neural information processing systems*, 6.

Davison, M. (2011). *Pharmaceutical anti-counterfeiting: combating the real danger from fake drugs*. John Wiley & Sons.

Duffner, S., Garcia, C., Idrissi, K., and Baskurt, A. (2021). Similarity metric learning. In *Multi-faceted Deep Learning*, pages 103–125. Springer.

He, K., Zhang, X., Ren, S., and Sun, J. (2016). Deep residual learning for image recognition. In *IEEE Conference on Computer Vision and Pattern Recognition, CVPR 2016, Las Vegas, NV, USA, June 27-30, 2016*, pages 770–778. IEEE Computer Society.

Joshi, S., Saxena, S., and Khanna, N. (2020). Source printer identification from document images acquired using smartphone. *arXiv preprint arXiv:2003.12602*.

Kipphan, H. (2001). *Handbook of print media: technologies and production methods*. Springer Science & Business Media.

Nguyen, Q.-T., Mai, A., Chagas, L., and Reverdy-Bruas, N. (2021). Microscopic printing analysis and application for classification of source printer. *Computers & Security*, 108:102320.

Schraml, R., Debiasi, L., Kauba, C., and Uhl, A. (2017). On the feasibility of classification-based product package authentication. In *Information Forensics and Security (WIFS), 2017 IEEE Workshop on*, pages 1–6. IEEE.

Schraml, R., Debiasi, L., and Uhl, A. (2018). Real or fake: Mobile device drug packaging authentication. In *Proceedings of the 6th ACM Workshop on Information Hiding and Multimedia Security*, pages 121–126. ACM.

Simonyan, K. and Zisserman, A. (2015). Very deep convolutional networks for large-scale image recognition. In *3rd International Conference on Learning Representations, ICLR 2015, San Diego, CA, USA, May 7-9, 2015, Conference Track Proceedings*.

Tkachenko, I., Trémeau, A., and Fournel, T. (2019). Authentication of medicine blister foils: Characterization of the rotogravure printing process. In *VISIGRAPP (4: VISAPP)*, pages 577–583.

Tkachenko, I., Trémeau, A., and Fournel, T. (2020). Fighting against medicine packaging counterfeits: rotogravure press vs cylinder signatures. In *2020 IEEE International Workshop on Information Forensics and Security (WIFS)*, pages 1–6. IEEE.

Tkachenko, I., Trémeau, A., and Fournel, T. (2022). Authentication of rotogravure print-outs using a regular test pattern. *Journal of Information Security and Applications*, 66:103133.

Tsai, M.-J., Tao, Y.-H., and Yuadi, I. (2019). Deep learning for printed document source identification. *Signal Processing: Image Communication*, 70:184–198.

Weinberger, K. Q., Blitzer, J., and Saul, L. (2005). Distance metric learning for large margin nearest neighbor classification. *Advances in neural information processing systems*, 18.